

AD-A086 427

IMPERIAL COLL OF SCIENCE AND TECHNOLOGY LONDON (ENGLAND) F/G 11/6
THE ROLE OF HYDROGEN IN THE STRESS CORROSION FAILURE OF HIGH ST--ETC(U)
APR 80 L CHRISTODOULOU, M G LACKEY DA-ER0-77-G-011

UNCLASSIFIED

NL

[OF]
40
AD-A086 427

END
DATE
FILMED
8-80
DTIC

ADA086427

LEVEL

A052407

12

The Role of Hydrogen in the Stress Corrosion Failure of
High Strength Al-Zn-Mg Alloys and Sensitised Austenitic
Stainless Steels.

Annual Technical Report

By

L. Christodoulou, M.G. Lackey, H.M. Flower, F.J. Humphreys
and P.R. Swann

April, 1980

EUROPEAN RESEARCH OFFICE

United States Army

London England

GRANT NUMBER DA-ERO-77-G-011

Imperial College

DTIC
ELECTE
JUL 7 1980
S D C

Approved for Public Release: distribution unlimited.

FILE COPY

80 7 2 010

UNCLASSIFIED

SECURITY CLASSIFICATION OF THIS PAGE (When Data Entered)

R&D 2374-MS

REPORT DOCUMENTATION PAGE		READ INSTRUCTIONS BEFORE COPYING
1. REPORT NUMBER	2. GOVT ACCESSION NO.	3. RECIPIENT'S CATALOG NUMBER
6 TITLE (and Subtitle) The Role of Hydrogen in the Stress Corrosion Failure of High Strength Al-Zn-Mg alloys and Sensitised Austenitic Stainless Steels.		9 5. TYPE OF REPORT & PERIOD COVERED Annual Technical Report, (Final),
10 7. AUTHOR(s) L./Christodoulou, M.G./Lackey, H.M./Flower F. J./Humphreys, P.D./Swann		6. CONTRACT OR GRANT NUMBER(s) 15 DAERC77-G-011
9. PERFORMING ORGANIZATION NAME AND ADDRESS Imperial College of Science & Technology Prince Consort Road London SW7		10. PROGRAM ELEMENT PROJECT, TASK AREA & WORK UNIT NUMBER 6.11.02A/1T161102BH-57-04 16
11. CONTROLLING OFFICE NAME AND ADDRESS USARDSG-UK Box 65 FPO NY 09510		12. REPORT DATE 11 April 1980
14. MONITORING AGENCY NAME & ADDRESS (if different from Controlling Office)		13. NUMBER OF PAGES 38 1238
		15. SECURITY CLASS. (of this report) Unclassified
15a. DECLASSIFICATION/DOWNGRADING SCHEDULE		
16. DISTRIBUTION STATEMENT (of this Report) Approved for Public Release Distribution Unlimited		
17. DISTRIBUTION STATEMENT (of the abstract entered in Block 20, if different from Report)		
18. SUPPLEMENTARY NOTES		
19. KEY WORDS (Continue on reverse side if necessary and identify by block number) (u) Stress Corrosion cracking (u) Al alloys (u) Stainless steels (u) Sensitization (u) Cr depletion (u) High Voltage microscopy		
20. ABSTRACT (Continue on reverse side if necessary and identify by block number) An investigation into the effect of exposure of Al-Zn-Mg alloys to water vapour has shown that hydrogen, produced by the reaction is absorbed by both the alloy grain boundaries and matrix. The amount of absorbed hydrogen depends on the local chemistry and the metal/Oxide interface and is influenced by alloying additions. Attainment of a critical concentration of dissolved hydrogen in the boundaries leads to brittle intergranular fracture on the subsequent application of stress.		

DD FORM 1 JAN 73 1473

EDITION OF 1 MAR 65 IS OBSOLETE

UNCLASSIFIED

SECURITY CLASSIFICATION OF THIS PAGE (When Data Entered)


UNCLASSIFIED

SECURITY CLASSIFICATION OF THIS PAGE (When Data Entered)

20. Continued.../

Attainment of a critical hydrogen concentration in the matrix leads to transgranular cleavage fracture.

Depending upon the alloy composition and heat treatment bubbles of gaseous hydrogen can be formed at suitable sites within the alloys such as grain boundary particles. The formation of grain boundary bubbles reduces embrittlement by reducing the local concentration of dissolved hydrogen.

It is proposed that the interaction of stress and environmental variables with the above criteria governs the environmental failure of Al-Zn-Mg alloys in aqueous and water vapour containing environments. It is suggested that such failures are hydrogen embrittlement dominated. 

The stress corrosion behaviour of sensitised austenitic stainless steel in dilute $H_2SO_4 + NaCl$ environments has been examined. Quantitative microanalysis of sensitised Type 304 steel has revealed that there is a depletion of Chromium in the vicinity of sensitised grain boundaries which can explain the susceptibility of the material to intergranular attack. This depletion, however, also results in the formation of martensite at the grain boundary. Results obtained to date indicate that a hydrogen embrittlement mechanism may be operating during the propagation of the intergranular stress corrosion crack.

Accession For	
NTIS GEM&I	<input checked="checked" type="checkbox"/>
DDC TAB	<input type="checkbox"/>
Unannounced	<input type="checkbox"/>
Justification	
By _____	
Distribution/	
Availability Codes	
Dist.	Avail and/or special
A	

UNCLASSIFIED

SECURITY CLASSIFICATION OF THIS PAGE (When Data Entered)

ABSTRACT

An investigation into the effect of exposure of Al-Zn-Mg alloys to water vapour has shown that hydrogen, produced by the reaction is absorbed by both the alloy grain boundaries and matrix. The amount of absorbed hydrogen depends on the local chemistry at the metal/oxide interface and is influenced by alloying additions. Attainment of a critical concentration of dissolved hydrogen in the boundaries leads to brittle intergranular fracture on the subsequent application of stress. Attainment of a critical hydrogen concentration in the matrix leads to transgranular cleavage fracture.

Depending upon the alloy composition and heat treatment bubbles of gaseous hydrogen can be formed at suitable sites within the alloys such as grain boundary particles. The formation of grain boundary bubbles reduces embrittlement by reducing the local concentration of dissolved hydrogen.

It is proposed that the interaction of stress and environmental variables with the above criteria governs the environmental failure of Al-Zn-Mg alloys in aqueous and water vapour containing environments. It is suggested that such failures are hydrogen embrittlement dominated.

The stress corrosion behaviour of sensitised austenitic stainless steel in dilute $\text{H}_2\text{SO}_4 + \text{NaCl}$ environments has been examined. Quantitative microanalysis of sensitised Type 304 steel has revealed that there is a depletion of Chromium in the vicinity of sensitised grain boundaries which can explain the susceptibility of the material to intergranular attack. This depletion, however, also results in the formation of martensite at the grain boundary. Results obtained to date indicate that a hydrogen embrittlement mechanism may be operating during the propagation of the intergranular stress corrosion crack.

CONTENTS

	PAGE
INTRODUCTION	1
Part 1. Aluminium-Zinc-Magnesium Alloys	2
1. Introduction	2
2. Summary of Results and Conclusions	4
Part 11. Austenitic Stainless Steel	7
1. STEM Microanalysis	7
2. Intergranular Stress Corrosion Cracking	10
3. Discussion and Conclusions	11
References	14
Tables	17
Figures	18

INTRODUCTION

This final report summarises the work performed over three years on the environment sensitive failure of high strength Al-Zn-Mg alloys, and the research carried out over two years on the intergranular stress corrosion cracking of sensitised austenitic stainless steels. The report is divided into two parts, covering each of the materials investigated.

I. Aluminium-Zinc-Magnesium Alloys

1. INTRODUCTION

The mechanism of environment-sensitive fracture in high strength aluminium alloys is subject to controversy at the present time. In spite of the very extensive past research into the metallurgical, mechanical and environmental aspects of the phenomenon there is no consensus as to the mechanism involved.

Two basic and fundamentally different mechanisms of failure have been advanced. The first, and perhaps most widely accepted, identifies the process of failure as one of a highly localised anodic dissolution reaction under the combined influence of stress and environment. The alternative model postulates that the phenomenon is controlled by a hydrogen embrittlement event. Hydrogen is believed to be generated as a consequence of the alloy/environment interaction, absorbed into the alloy and be responsible for the brittle fracture event.

Many variations on the basic theme of electrochemical dissolution introduced by E.H. Dix in the "1949 Edward DeMille Campbell Memorial Lecture" (Trans. A.S.M. Vol.42 p.1057 1950) have been presented in the intervening years and many workers have interpreted their results via the dissolution control models. These vary from the metallurgically biased preferential dissolution of grain boundary precipitates(1) or precipitate free zones (2) through oxide film rupture and dissolution (3-7), including effects of coplanar slip (8, 9) models, to theories of stress (10) or strain (3) assisted dissolution. Similarly a range of hydrogen embrittlement theories have been extended to Al-Zn-Mg alloys from other systems covering such concepts as hydrogen adsorption (11) hydrogen absorption (12) and void pressurisation (13).

A view that is rapidly gaining support among many workers is the one that considers that both dissolution and hydrogen mechanisms (with the appropriate modifications for any one system under consideration) can operate either in parallel or in competition. Certainly the available literature would not contradict such a view.

The aims of the current study were to examine the condi-

tions of generation, entry and effect of hydrogen on the environment-sensitive fracture event in a water vapour environment and to establish the mechanism of failure. It was further proposed to assess the potential of any developed mechanism to explain other results reported in the literature.

The study has been confined to three alloys based on the Al-Zn-Mg system (7000 series alloys). A high purity Al-6% Zn- 3% Mg alloys was examined together with two quaternary compositions, based on the above, containing copper and chromium additions respectively.

The investigation has been largely based on electron microscopical techniques. Both standard and specialised transmission electron microscopy techniques were employed to study the alloy/environment interaction. In particular, "in-situ" high voltage electron microscopy was used extensively to monitor directly the reaction of the experimental alloys with water vapour, both in the presence and absence of stress. The technique was shown to be a most powerful tool of investigation and furnished direct evidence of hydrogen penetration into Al-Zn-Mg alloys.

Susceptibility to embrittlement was assessed by extensive mechanical testing of samples exposed to water vapour and fractographic studies using high resolution scanning electron microscopy.

On the basis of the presented results a model of failure, derived from previous proposals (14,15) was developed. In its basic form it is capable of explaining many of the observed phenomena. It indicates that an absorbed hydrogen embrittlement mechanism can satisfactorily explain the environmental failure behaviour of Al-Zn-Mg alloys under most conditions.

2. SUMMARY OF RESULTS AND CONCLUSIONS

It has been demonstrated in this work that exposure of Al-Zn-Mg alloys to water vapour containing environments leads to the formation of hydrogen and its subsequent introduction into the alloys. It has also been shown that under particular conditions the absorbed hydrogen can lead to severe embrittlement of both grain boundaries and matrix.

The overall hydrogen embrittlement phenomenon depends on two factors.. It is sensitive to the surface reaction events which govern the entry of hydrogen and to the inherent tolerance of the alloy microstructure to its presence. Modification of one or both of these factors by metallurgical, environmental or stress variables results in a change in the environment-sensitive failure characteristics of the alloys. Specifically the following conclusions have reached:

- 1) As a consequence of the exposure of the alloys to water vapour hydrogen is generated at the metal/oxide interface. This leads to oxide decohesion and blistering.
- 2) The reaction leads to the establishment of a duplex oxide at the surface of the metal consisting of an outer layer of pseudoboehmite (AlOOH) and an inner, very thin layer of amorphous oxide. Eventually bayerite ($\text{Al}(\text{OH})_3$) is formed.
- 3) Growth of the oxyhydroxide phase occurs via a co-operative process of inward diffusion of water through the outer layer and an ionic transfer process across the inner amorphous film. Outward diffusion of aluminium ions through the amorphous layer is compensated by the inward diffusion of protons.
- 4) Pseudoboehmite growth occurs by transformation of the oxide and not by a dissolution-precipitation process.
- 5) The surface reaction is enhanced by electron irradiation. ionisation damage is responsible for the acceleration of the reaction.
- 6) The cooperative action of ionisation damage and water vapour is necessary for the acceleration of the reaction to occur.
- 7) Significant hydrogen penetration of the alloys is achieved as a result of the alloy/water reaction.
- 8) The amount of hydrogen introduced into the samples is affected by minor alloying elements. Specifically chromium

additions reduce the amount of absorbed hydrogen by catalysing the formation of gaseous hydrogen at the interface and its subsequent evolution into the atmosphere.

9) Hydrogen is absorbed into the matrix and grain boundaries of the alloy. A hydrogen concentration profile is established in both.

10) The hydrogen profile in the grain boundaries is shallow and results from a high hydrogen grain boundary mobility. In contrast the matrix profile is steep.

11) The attainment of a critical hydrogen concentration of dissolved hydrogen in the boundaries leads to brittle intergranular failure. Similarly the attainment of a critical hydrogen concentration in the matrix leads to transgranular cleavage fracture.

12) The presence of the critical hydrogen concentration in solution at the grain boundaries causes a reduction of grain boundary surface energy of approximately 90%. It is this criterion that controls the susceptibility of the alloy to embrittlement and environment-sensitive failure.

13) Molecular hydrogen 'bubbles' are formed at the grain boundaries of exposed samples. They act as beneficial traps for the absorbed hydrogen reducing the local concentration in solution. They can however act as brittle crack nuclei in an embrittled grain boundary.

14) Formation of bubbles greatly increases the resistance of the alloys to embrittlement. Overaged alloys owe their resistance to embrittlement to the ability of the grain boundary precipitates to form hydrogen bubbles.

15) In the ternary Al-6%Zn-3%Mg and quaternary Al-6%Zn-3%Mg-0-14%Cr alloys hydrogen bubbles are formed preferentially on grain boundary particles under the experimental conditions employed.

16) An addition of 1.7% copper to the ternary alloy markedly stimulates the formation of grain boundary bubbles, even in the absence of grain boundary precipitates. This is the primary reason for the increased resistance to embrittlement by the 6/3 Cu alloy.

17) The nucleation and growth of grain boundary hydrogen bubbles is restricted by the resistance offered by the immediately adjacent matrix regions.

18) There exists a hydrogen/dislocation association. It is possible that this association leads to an interference of normal glide processes.

19) The intimate relationship between pre-exposure embrittlement and aqueous stress corrosion cracking strongly suggests that the environment-sensitive failure of Al-Zn-Mg alloys is determined by a hydrogen embrittlement mechanism. The effects of metallurgical environmental and stress variables can be rationalised by their influence on the local hydrogen entry processes and the internal tolerance of any one system to the presence of hydrogen.

20) Finally it is concluded that "in-situ" high voltage electron metallography offers a unique technique of studying the environmental degradation and failure of Al-Zn-Mg alloys. Provided adequate account of possible atypical results is taken the technique has the potential to offer a great many insights into the environment sensitive failure of high strength aluminium alloys.

During the period covered by this report the work has led to the publication of two papers in the research literature (16,17).

II. Austenitic Stainless Steel

1. STEM MICROANALYSIS

Heat treatment of austenitic stainless steel in the temperature range 500°C-800°C results in the precipitation of chromium-rich carbides ($M_{23}C_6$ type) along grain boundaries with concomitant depletion of Cr in the grain boundary region. The susceptibility of the material to intergranular attack has been attributed to the existence of a zone adjacent to the grain boundary where the chromium content is less than 12 wt.%.¹⁸ Although the presence of the chromium depleted zone has been indirectly observed, existing analytical tools have been unsuccessful in detecting this very small region ($\sim 1500 \text{ \AA}$).

By combining STEM with energy dispersive spectrometry, the spatial resolution obtainable for microanalytical purposes has been significantly improved. The fine probe sizes available in STEM (20-200 \AA) result in a spatial resolution of several hundred angstroms in thin-foil microanalysis. Of paramount importance is the applicability of STEM to quantitative microanalysis of thin-foil specimens. For electron-transparent specimens (50-200nm), the analysed volume is determined to a great extent by the diameter of the incident electron probe.

A technique for quantitative analysis using the ratio of characteristic X-ray peak intensities has been described by Cliff and Lorimer 19:

$$\frac{C_A}{C_B} = K_B^A \frac{I_A}{I_B}$$

where : C_A, C_B = compositions of elements A, B (wt.%)

I_A, I_B = characteristic intensities of elements A,B.

K_B^A = proportionality constant

This is generally suitable for thin foil specimens (electron transparent at 100kV) which do not exhibit significant X-ray absorption and fluorescence effects (Philibert "thin film" approximation).^{20, 21}

Experimental Technique :

Analyses were conducted using a JEOL 120 CX STEM/TEM equipped with Link Energy Dispersive X-ray Microanalysis facilities. The operating voltage was 100kV and the probe diameter employed was approximately 200Å. Beam spreading was calculated to be 300Å, however the contamination spots produced during analysis (~500Å diameter) were taken as the extent of the analysed area. The count time for each analysis was 100 seconds. All specimens were tilted $\sim 40^\circ$ towards the detector for optimised X-ray collection. Only boundaries which were parallel with the incident electron beam were analysed.

Material :

3.0mm diameter discs of type 304 steel were solution-annealed at 1120°C for $\frac{1}{2}$ -hour, water quenched and subsequently sensitised at 675°C or 600°C . All heat treatments were conducted in vacuo. A range of sensitisation times (15 mins to 100 hrs) were examined so that the effect of sensitisation treatment on the Cr concentration profile at the grain boundaries could be determined.

The composition of the steel studied in this investigation is presented in Table 1.

Thin foils were prepared from the 3.0mm discs by jet polishing at room temperature in a 95% Acetic-5% Perchloric Acid solution at 60V.

Results and Discussion:

The results of the spot analyses at sensitised grain boundaries are presented in Figures 1 and 2. The composition determined from the analysis is taken as the average composition over a cylinder $\sim 500 \text{ \AA}$ in diameter and 150 \AA in height (foil thickness). Error bars on the individual analyses represent one standard deviation.

It was found that no unique solute profile could adequately characterise a particular sensitisation treatment;

rather a range of solute profiles were obtained for each treatment examined. This illustrates the importance of grain boundary misorientation and the degree of precipitation on the extent of the Cr-depleted zone. The Cr-profiles obtained in Figures 1 and 2 represent the most severe depletions which were detected for a given heat treatment. Figure 3 contains representative solute profiles from coherent and incoherent twin boundaries.

The width of these depleted zones are in reasonable agreement with those predicted by Stawström and Hillert²². As expected, the extent of the zone increases as sensitisation time and temperature increases. It was not possible to confirm the assumption of Tedmon et al.²³ regarding the minimum Cr content at the carbide interface, as the minimum diameter of the analysed volume was $\sim 500 \text{ \AA}$. However, in the 675°C long-term sensitisation treatments, the minimum Cr-content measured over a grain boundary between carbides was $9.5 \pm .5\%$ Cr (over a $\sim 500 \text{ \AA}$ diameter area). This represents a lower value of Cr-content than that predicted by Tedmon et al.²³ in their analysis of the sensitisation process.

Using the widths of the depleted zones, it was possible to evaluate the diffusivity of Cr in γ . The experimental values of D_{Cr} were in good agreement with the diffusion data of Stawström and Hillert²².

Solute profiles across some sensitised boundaries were asymmetric, i.e. the Cr concentration profile in Figure 4. This asymmetry is related to the nature of the grain boundary carbides. M_{23}C_6 is generally semi-coherent with one of the austenite grains²⁴. The carbide exhibits a cube-cube orientation relationship with the austenite $(100)_{\text{M}_{23}\text{C}_6} \parallel (100)_\gamma$ and $[100]_{\text{M}_{23}\text{C}_6} \parallel [100]_\gamma$ ²⁵. The wider depleted zone exists adjacent to the incoherent $\text{M}_{23}\text{C}_6/\gamma$ interface. It is generally assumed that the solute is transported to the carbide via volume diffusion to the grain boundary, and grain boundary diffusion to the growing carbide. The experimentally determined solute profiles indicate that this does occur in the grain on the incoherent side of the precipitate, but that volume diffusion is not the controlling process in the grain which is semi-coherent with the carbide. Figure 5 depicts a grain boundary that exhibits

an asymmetrical solute profile. It is probable that the growth of the carbide on the semi-coherent side is interface-controlled, and that a ledge mechanism may be operating.

The second part of this investigation dealt with evaluating the IGSCC behaviour of the sensitised austenitic stainless steel :

2. INTERGRANULAR STRESS CORROSION CRACKING

Material:

Miniature tensile specimens were machined from 0.50mm sheet, and subsequently solution-annealed in vacuo at 1120°C and water quenched. The solution-annealed specimens were then sensitised in vacuo at 675°C for periods of 2 to 72 hours. After sensitisation, the specimen gauge lengths were electropolished in 95% Acetic-5% Perchloric Acid at 30V.

Environment:

After considerable experimentation, it was found that dilute $H_2SO_4/NaCl$ solutions successfully promoted intergranular cracking at room temperature without causing significant general corrosion, in contrast with the solutions used by Hartson & Scully²⁶. The solution employed in this investigation was 0.12M H_2SO_4 + 0.024M NaCl(pH=1). Additional testing was conducted in more dilute environments - pH=2 to 5.

Testing :

The stress corrosion behaviour of sensitised type 304 steel was evaluated through slow strain-rate testing. All tests were conducted on an Instron Tension machine at a strain rate of $10^{-6} \text{ sec.}^{-1}$. (The exact experimental set-up has been described in a previous report). After testing, fractured specimens were prepared for metallographic examination.

Results :

The results of the stress corrosion tests indicate that the susceptibility of the sensitised specimens to IGSCC is related to the degree of sensitisation, with the 72hr. sensitisation treatment exhibiting the greatest susceptibility. As the pH was

increased, ductility parameters also increased. These results are presented in Figure 6.

In the most acidic environments, the fracture mode was predominantly intergranular. A small area of intergranular tearing was observed where the final failure occurred. Micrographs A and B in Figure 7 are typical of the fracture surfaces in these specimens. The lightly sensitised specimens exhibited some intergranular fracture, but the dominant failure mode was microvoid coalescence (Figure 8).

Although the highly acidic environments did not promote substantial general attack, there was considerable evidence of dissolution on some stress corroded surfaces. Slip line attack and pitting were frequently observed in the pH=1 solutions, as shown in Figure 7. The occurrence of dissolution of the fracture surfaces complicates a valid interpretation of the fractography in terms of a fracture mechanism. As demonstrated previously, the Cr-content of the austenite adjacent to the sensitised grain boundaries can fall below the 12 wt.% necessary for the formation of a passive Cr_2O_3 film. Therefore, it would be expected that after the stress corrosion crack has advanced (by a hydrogen embrittlement and/or anodic dissolution mechanism), the exposed surfaces behind the crack would be readily attacked by the solution. By employing less acidic solutions (pH=2-4), this additional dissolution of the fracture surfaces was reduced considerably.

3. DISCUSSION AND CONCLUSIONS

The fact that sensitisation results in the development of a Cr-depleted zone adjacent to the (high-angle) grain boundaries, taken with the results of the SCC tests, is not consistent with a dissolution mechanism. If the existence of the Cr-depleted austenite is sufficient for intergranular SC failure by a dissolution mechanism, all of the specimens examined should have failed intergranularly, for there would be a relatively continuous depleted zone. Clearly, this did not occur, which tends to suggest that another SCC mechanism(s) may be operating.

Examination of thin-foils from stress-corroded and strained specimens in the TEM revealed the existence of somewhat irregular bands of both martensite (Figure 9). Quantitative microanalysis confirmed that the Cr-content in this region was within the compositional limits for massive martensite (<16 wt.% Cr)²⁷. Further examination has shown that not all boundaries form martensite, which is in agreement with the quantitative microanalysis of the specimens sensitized under various conditions. Martensite formation appears to be very dependent upon the nature of the Cr-concentration profile (and thus the particular sensitisation treatments) and grain boundary. The solute profile in Figure 10 was conducted across a transformed zone. A significant change in Cr content was detected on either side of the α'/γ interface. It was also observed that the amount of martensite formed along either side of the boundary is not necessarily equal. This is additional support of the microanalytical results which indicate an asymmetry of the Cr profile.

Dissolution models for intergranular SCC in sensitised austenitic stainless steel ignore the preferential formation of martensite along sensitised grain boundaries. A hydrogen embrittlement mechanism of SCC in martensitic steels, however, is widely accepted. The existence of this martensite merits serious consideration of a possible hydrogen embrittlement mechanism for SCC in this material. Evidence of the susceptibility of sensitised Type 304 stainless steel to hydrogen embrittlement has been presented by Briant²⁸. Briant has also indirectly observed the existence of a α' in stress-corroded specimens.

The fact that this material exhibits intergranular stress corrosion cracking at elevated temperatures has been used to discount possible hydrogen embrittlement of the α' . The α' in the Cr-depleted zone is formed as a result of the increase in M_s ²⁹ (approximately 30°C for each wt.% Cr decrease) and M_d . This α' , once formed, is stable up to $\sim 500^\circ\text{C}$ when reversion occurs.

Research is in progress to clarify the role of this preferential grain boundary martensite in terms of a hydrogen

embrittlement mechanism or combined hydrogen and dissolution mechanism for intergranular SCC in sensitised 304 stainless steel. Results obtained to date strongly suggest that a hydrogen embrittlement mechanism is dominant in the IGSCC of this material in dilute $\text{H}_2\text{SO}_4/\text{NaCl}$ environments.

REFERENCES

1. P.K. Poulou, J.E. Morral and A.J. McEvily.
Met. Trans. 5, 1393, 1974.
2. G. Thomas and J. Nutting.
J. Inst. Metals. 88, 81, 1959-60
3. T.P. Hoar.
Proc. Conf. on "Fundamental Aspects of Stress Corrosion
Cracking" N.A.C.E. Columbus. Ohio, 98, 1969
4. H.L. Hogan.
"The Stress Corrosion of Metals". Wiley N.Y. 1966
5. D.A. Vermilyea.
J. Electrochem. Soc. 119, 405, 1972
6. T.P. Hoar and F.P. Ford.
J. Electrochem. Soc. 120, 1013, 1973
7. J.C. Scully.
Corrosion Science. 7, 197, 1967
8. H.A. Hall
Corrosion. 23, 173, 1967
9. T. Kawabata and O. Izumi.
J. Mat. Sci. 14, 1071, 1979
10. M.G. Creager and P.C. Paris.
Inst. J. Fracture Mechanisms. 3, 247, 1967
11. N.J. Petch and P. Stables,
Nature, 169, 824, 1952
12. R.A. Oriani.
Berichte der Bunsengen Sur Phys.Chem. 76, 848, 1972
13. H.P. Van Leeuwen.
Corrosion 29, 197, 1973
14. L. Montgrain and P.R. Swann.
Proc. Int. Conf. on Hydrogen in Metals. Metals
Ohio, 1974 p.375
15. G.M. Scamans, R. Alani and P.R. Swann
Corrosion Science, 16, 443, 1976

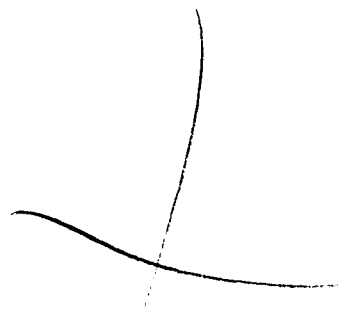
16. L. Christodoulou and H.M. Flower
"Electron Microscopy and Analysis 1979" . Inst. Phys.
Conf. S No 52, 1980 p.313
17. L. Christodoulou and H.M. Flower
Acta Met. 28, 481, 1980
18. E.C. Bain, R.H. Aborn and J.J.B. Rutherford
Trans Amer. Soc. Steel Treating, 21, 481, 1933
19. G. Cliff and G.W. Lorimer
J. Microscopy, 103, 203, 1975
20. J. Bentley and E.A. Kenick
Scripta Met., 11, 261, 1977
21. C. Nockolds, M.J. Nasir, G. Cliff and G.W. Lorimer
Electron Microscopy and Analysis 1979, Inst. Phys.
Conf. S No. 52, 1980 p.417
22. C. Stawström and M. Hillert
JISI, 207, 77, 1969
23. C.S. Tedmon, Jr., D.A. Vermilyea and J.H. Rosolowski
J. Electrochem. Soc., 118, 192, 1971
24. L.K. Singhal and J.W. Martin
Trans. Met. Soc., AIME, 242, 814, 1968
25. M.H. Lewis and B. Hattersley
Acta Met., 13, 1159, 1965
26. J.D. Hartson and J.C. Scully
Corrosion, 25, 493, 1969
27. S. Floreen
Trans. Met. Soc. AIME, 236, 1429, 1966

28. C.L.Priant
Met.Trans, 9A, 731, 1978
29. E.P. Butler, M.G. Lackey, and K.B. Guy
6th Int'l Conf. on HVEM (Antwerp, 1980) to be published.

TABLE I.

Composition of Type 304 Steel (wt. %)

C	Mn	Cr	Ni	P	S	Si	Mo	Al	Cu
0.7	1.55	19.0	9.0	.025	.03	.54	.25	13	.23



Blank

Figure 1. Chromium Concentration Profiles

These profiles represent the most severe depletion detected at grain boundaries for each specific heat treatment at 675°C.

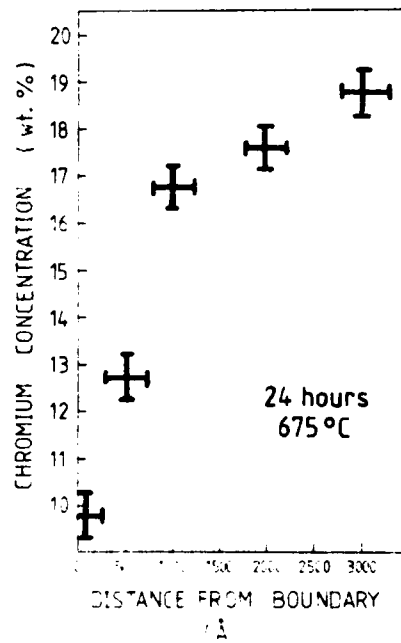
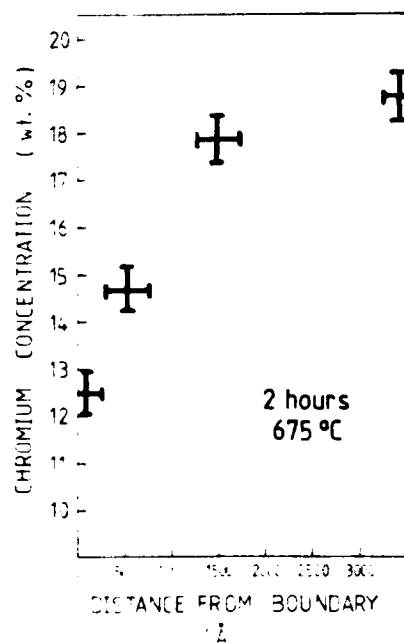
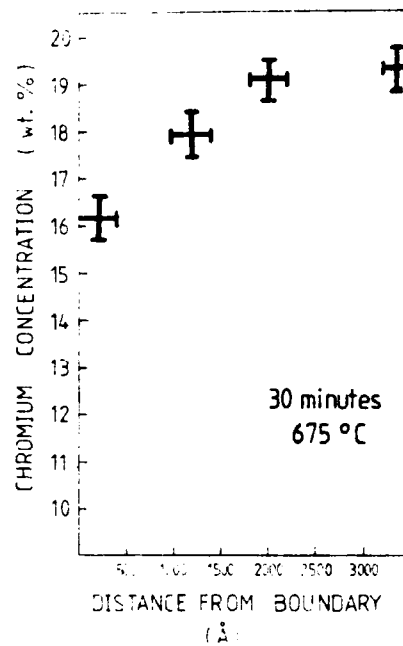
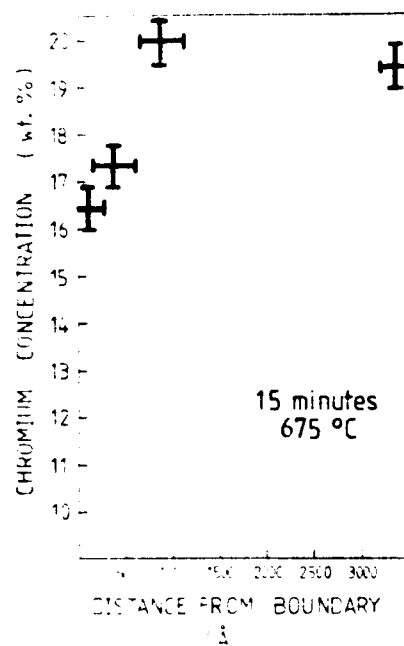


Figure 1.

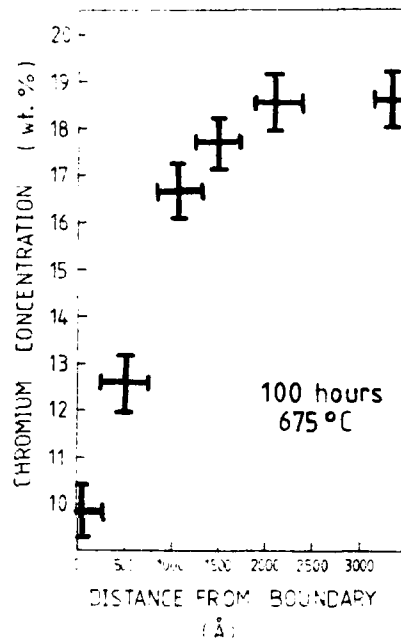
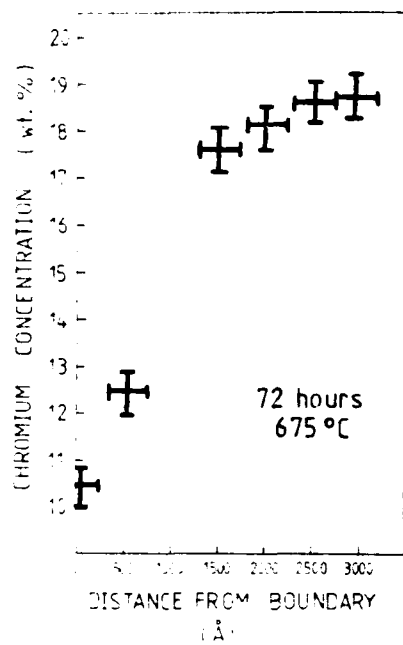


Figure 1. continued

Figure 2. Chromium Concentration Profiles

These profiles depict the most severe depletion detected at grain boundaries for heat treatments of 2, 24 and 72 hours at 600°C.

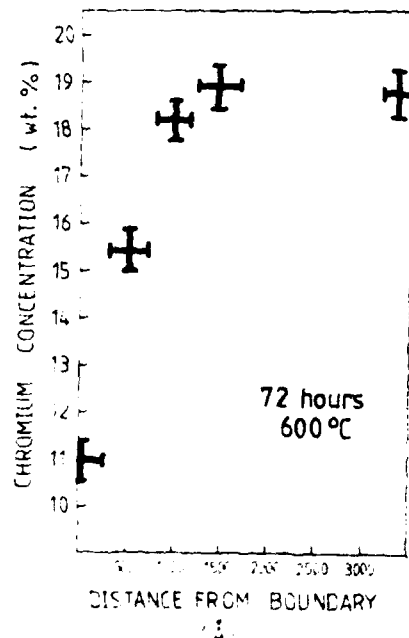
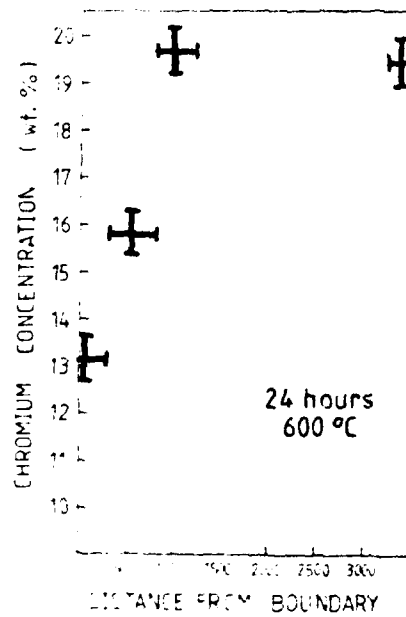
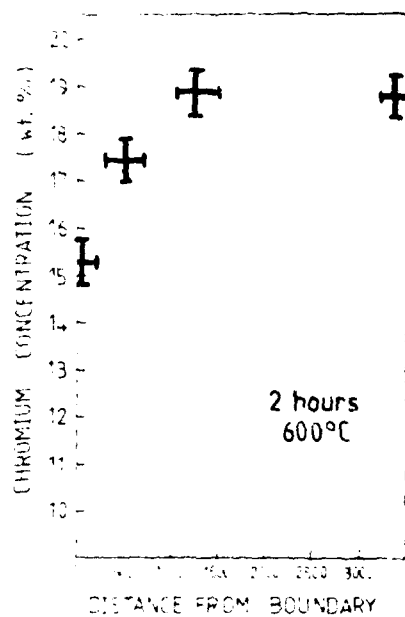
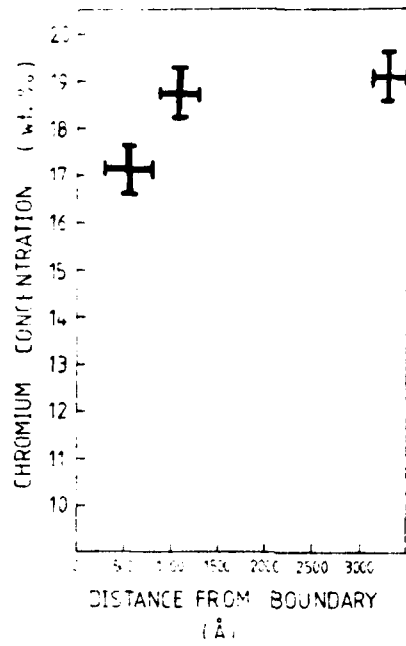


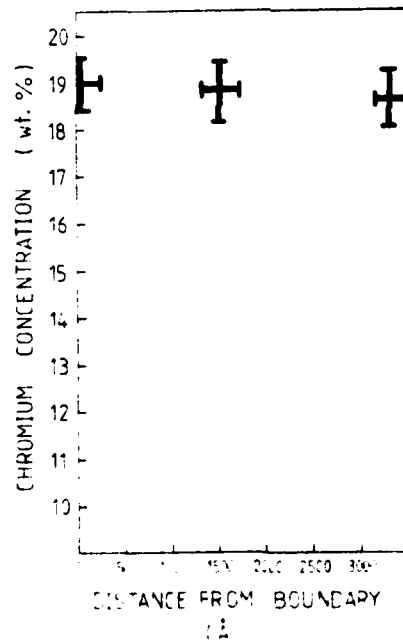
Figure 2.

Figure 3. Chromium Concentration Profiles

Profile 3A is representative of the solute depletion observed at incoherent twin boundaries after sensitising for 72 hours at 675°C. A typical Chromium profile at a coherent twin boundary is illustrated in 3B.



3 A.



3 B.

Figure 3.

Figure 4. Asymmetric Chromium Concentration Profile

This profile is representative of the asymmetric concentration gradient found when analysing across some grain boundaries. This particular profile was obtained from a specimen sensitised for 72 hours at 675°C.

Figure 5. Sensitised Grain Boundary

This type of microstructure was generally observed in conjunction with the asymmetric Chromium profile. The wider depleted zone was found to occur on the incoherent side of the carbides. The sensitisation treatment was 72 hours at 675°C.

72 hours at 675°C

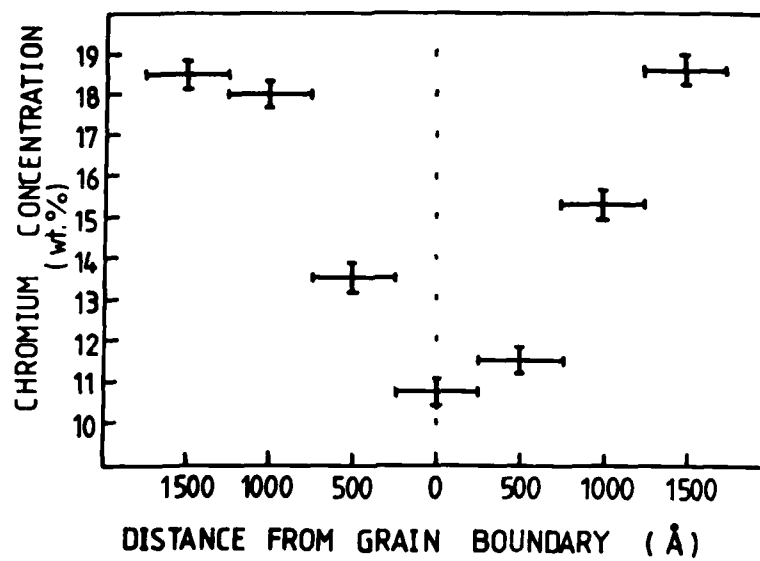


Figure 4.



Figure 5.

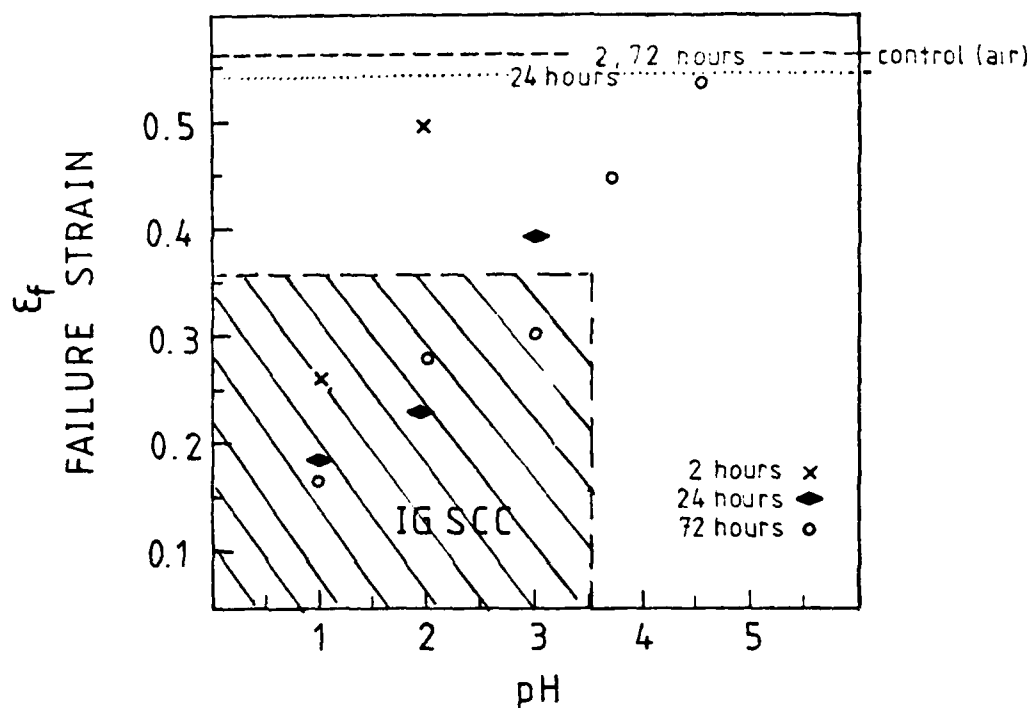


FIGURE 6.

Strain to failure vs. pH for specimens sensitised at 675°C.

Figure 7. Fractography of SCC

These fractographs are typical of the SCC observed in the more acidic solutions (pH=1, pH=2). Brittle intergranular fracture is depicted in Micrographs A and C, while intergranular tearing predominates in B. Slip line attack and pitting can also be seen in Micrograph C.



A.



B.

50 μ

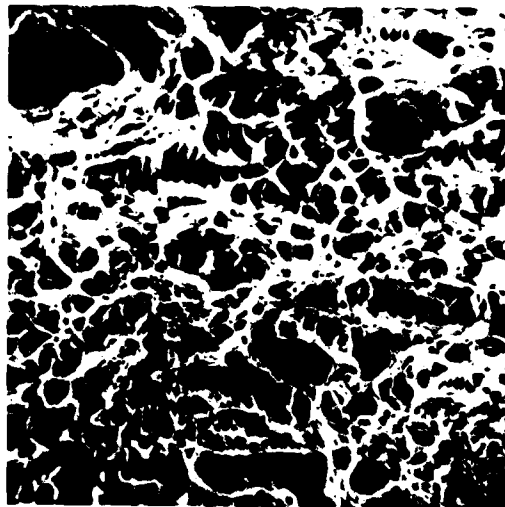


C.

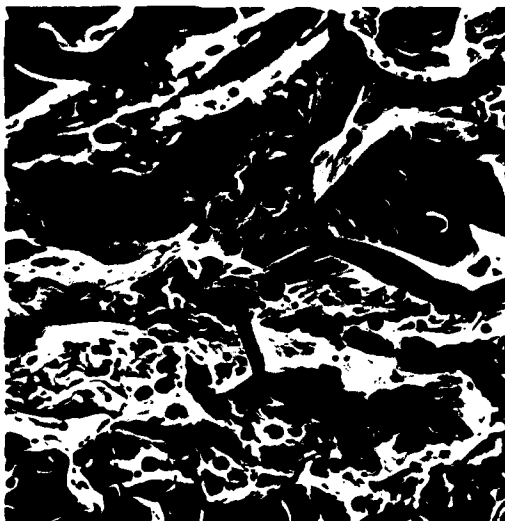
10 μ

Figure 7.

Figure 8. Representative Micrographs of
Lightly Sensitised (2 hours at
675°C) SCC specimens.



A. 50μ



B. 50μ

Figure 8.

Figure 9. Martensite in Sensitised 304.

Lath martensite was observed to form along certain grain boundaries. The particular sensitisation treatment in this instance was 72 hours at 675°C.

Figure 10. Chromium Concentration Profile
across Transformed Grain Boundary

From this concentration profile, it is evident that the lath martensite form within defined a compositional zone ($\%Cr \approx 16 \text{ wt}\%$). There is a distinct composition boundary at the α'/γ interface. The heat treatment for this specimen was 72 hours at 675°C.



Figure 9.

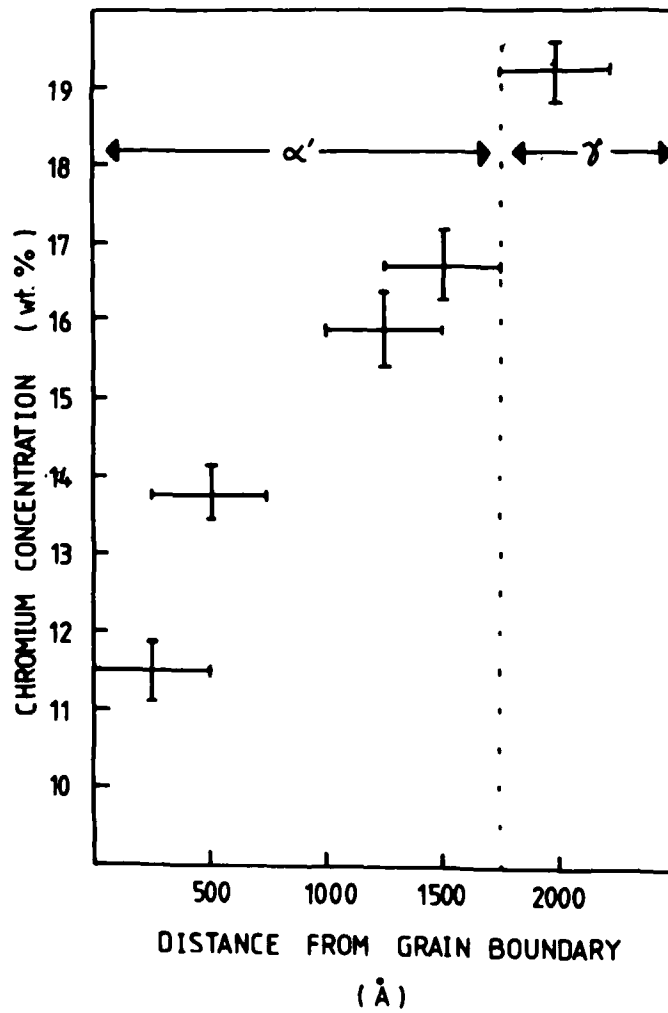


Figure 10.

